
Article:
Long, F., Harrison, P. and Hagston, W.E. (1996) Empirical pseudopotential calculations of Cd1-xMnxTe. Journal of Applied Physics, 79 (9). pp. 6939-6942. ISSN: 1089-7550

https://doi.org/10.1063/1.361519

Empirical pseudopotential calculations of $Cd_{1-x}Mn_xTe$

Fei Long
Department of Applied Physics, University of Hull, HU6 7RX, United Kingdom

P. Harrison[a)]
Department of Electronic and Electrical Engineering, University of Leeds, LS2 9JT, United Kingdom

W. E. Hagston
Department of Applied Physics, University of Hull, HU6 7RX, United Kingdom

(Received 10 October 1995; accepted for publication 16 January 1996)

Empirical pseudopotential calculations for the entire range of alloy concentrations of cubic $Cd_{1-x}Mn_xTe$ are presented. The atomic form factors have been deduced empirically by fitting the band structure to spectroscopic data available from the literature. The pseudopotential band structures indicate optical bowing may occur in the alloy $Cd_{1-x}Mn_xTe$ and have been used to determine the effective masses of the electron and light, and heavy holes, which for CdTe are in agreement with accepted values. The effective masses for $Cd_{1-x}Mn_xTe$ are given for the first time, and are expressed as first- and second-order polynomials in x. The implications of these results for spectroscopic experiments are discussed. © *1996 American Institute of Physics.* [S0021-8979(96)01609-9]

I. INTRODUCTION

Experimental and theoretical studies of the diluted magnetic semiconductor $Cd_{1-x}Mn_xTe$ in both bulk and multiple-quantum-well (MQW) samples have proven to be a very fruitful avenue of research due to the large sp^3-d exchange interaction between the carriers and the magnetic Mn^{2+} ions. When placed in a magnetic field the exchange interaction produces a giant Zeeman splitting in the conduction and valence bands. Theoretical studies[1,2] of this phenomenon have led to a greater understanding of the nature of this paramagnetism in all such diluted magnetic semiconductors (DMS). Furthermore, studies of MQW samples formed from CdTe wells separated by $Cd_{1-x}Mn_xTe$ barriers have led to an understanding of phenomena unique to heterostructures formed from DMS, such as ''two-dimensional'' magnetic polarons,[3] the magnetic-field-induced type-I–type-II transition,[4] and the enhanced paramagnetic behavior of the interfaces adjacent to nonmagnetic material.[5,6]

Despite this intensive study and the availability of high-quality samples, (for example, Jackson *et al.*[7] report photoluminescence linewidths for a $CdTe/Cd_{1-x}Mn_xTe$ MQW$\sim$1 meV), some of the fundamental parameters central to the theoretical models used to account for the behavior of $Cd_{1-x}Mn_xTe$ (the most common DMS) are either unknown or the subject of some debate. In particular, although the effective mass approximation is used extensively throughout the $CdTe/Cd_{1-x}Mn_xTe$ literature, the actual electron and hole effective masses are unknown within the magnetic alloy, as pointed out recently by Kuhn-Heinrich *et al.*[8] Similarly a wide variety of mass parameter values are employed for CdTe. In particular the heavy-hole effective mass along the growth (z) direction of a MQW has been assigned values ranging from 0.4 to $0.6m_0$.[8–11]

In order to understand fully the physics of this well-studied system it is essential that the input parameters to the models are known accurately. The purpose of this work is to use the highly successful empirical pseudopotential technique to calculate the full band structure of the range of alloys of $Cd_{1-x}Mn_xTe$ and hence determine the electron and light- and heavy-hole effective masses for all x. These values will then provide the necessary input to the more commonly used effective mass model.

II. THEORETICAL MODEL

The local empirical pseudopotential scheme is well known in the literature; see, for example, Ref. 12. The bulk eigenfunctions $\phi_{n,\mathbf{k}}$ within the time-independent Schrödinger equation

$$\mathscr{H}\phi_{n,\mathbf{k}}=E_{n,\mathbf{k}}\phi_{n,\mathbf{k}} \tag{1}$$

are expanded in terms of a linear combination of plane waves, i.e.,

$$\phi_{n,\mathbf{k}}=\frac{1}{\sqrt{\Omega}}\sum_{\mathbf{G}} a_{n,\mathbf{k}}(\mathbf{G})\exp[i(\mathbf{G}+\mathbf{k})\cdot\mathbf{r}], \tag{2}$$

where the Hamiltonian $\mathscr{H}$ is given by

$$\mathscr{H}=-\frac{\hbar^2}{2m_0}\nabla^2+\sum_{\mathbf{r}_a} V_a(\mathbf{r}-\mathbf{r}_a) \tag{3}$$

and the crystal potential is approximated by a spherically symmetric atomic potential V_a situated at every lattice site $\mathbf{r}_a$. This standard technique leads to a pseudopotential of the form

$$V=\sum_{|\mathbf{G}'-\mathbf{G}|}(V^S_{|\mathbf{G}'-\mathbf{G}|}\cos|\mathbf{G}'-\mathbf{G}|\cdot\mathbf{T}+iV^A_{|\mathbf{G}'-\mathbf{G}|} \times\sin|\mathbf{G}'-\mathbf{G}|\cdot\mathbf{T}), \tag{4}$$

where $\mathbf{T}=(1,1,1)a/8$. For the ternary system of $Cd_{1-x}Mn_xTe$ being studied here, the symmetric V^S and antisymmetric V^A form factors can be expressed by

a)Electronic mail: p.harrison@elec-eng.leeds.ac.uk

TABLE I. Atomic form factors of CdTe and cubic MnTe in Ryd. Note that the subscript for V represents $|\mathbf{G}'-\mathbf{G}|^2$.

	V_3^S	V_8^S	V_{11}^S	V_3^A	V_4^A	V_{11}^A
CdTe	−0.23	−0.005	0.081	0.12	0.0715	0.0385
MnTe	−0.225	−0.004	0.095	0.15	0.11	0.0075

$$V^{S,A}=\frac{(1-x)\Omega_{\mathrm{CdTe}}V^{S,A}_{\mathrm{CdTe}}+x\Omega_{\mathrm{MnTe}}V^{S,A}_{\mathrm{MnTe}}}{\Omega_{\mathrm{Cd}_{1-x}\mathrm{Mn}_x\mathrm{Te}}}, \tag{5}$$

where Ω is the volume of the (cubic) unit cell and the lattice constant of the ternary alloy is assumed to follow Vegard's rule

$$a_{\mathrm{Cd}_{1-x}\mathrm{Mn}_x\mathrm{Te}}=(1-x)a_{\mathrm{CdTe}}+xa_{\mathrm{MnTe}}. \tag{6}$$

The lattice constant for CdTe a_{CdTe} was taken as 6.481 Å and for zinc-blende MnTe $a_{\mathrm{MnTe}}=6.244$ Å.[13] Note that as the lattice constant is a function of the alloy concentration x, then the reciprocal lattice vectors $\mathbf{G}$ used in the expansion are also dependent upon x. Therefore the symmetric V^S and antisymmetric V^A form factors at lattice constants different from the natural lattice constants of CdTe and MnTe were obtained by a polynomial fit to V as a function of $|\mathbf{G}'-\mathbf{G}|$.

The model adopted for the spin-orbit interaction is the one originally introduced by Bloom and Bergstresser[14] and later described by Walter *et al.*[15] 169 plane waves of different $\mathbf{G}$ are used in our calculation and the dimension of the eigenvalue matrix doubles when spin-orbit interaction is included.

III. RESULTS

Pure CdTe has the zinc-blende structure, the form factors of which are determined empirically by adjusting them to produce the closest agreement between the calculated and experimentally observed band structure. As shown in Table I, our form factors are different from those of Cohen and Bergstresser.[12] This discrepancy could have arisen from the experimental data used in the present work.[16–18] Such data were not available to Cohen and Bergstresser and are indeed inconsistent with their band structure. Furthermore, the lattice constant and the number of plane waves used in the present calculations are also different. Although the present work adopts the local approach, the band structure obtained for CdTe, with the form factors of Table I, agrees well with that derived from the nonlocal pseudopotential calculation of Ref. 19, which itself is in good agreement with more recent experimental data.

Pure MnTe crystallizes in the single-phase hexagonal NiAs structure below 1040 °C.[20] Both experiment[21] and theory[13] have suggested that alloys of $\mathrm{Cd}_{1-x}\mathrm{Mn}_x\mathrm{Te}$ with manganese concentrations up to ~0.7 assume the single-phase zinc-blende structure. This means that the adamantine phase of MnTe exists in the alloy although it is not found in the phase diagram at the present time.

There exist in the literature several electronic structure calculations of MnTe in the hypothetical zinc-blende structure.[13,22,23] The present work, however, uses for the first time the empirical pseudopotential formalism. The form factors were obtained by fitting the band structure to the self-consistent local spin-density total energy calculation of Ref. 13. However, two important changes were made with regard to the Γ point of the Brillouin zone. The first is that the fundamental gap of MnTe was taken to be that given by experiment as deduced from the formula[18] with $x=1$, namely,

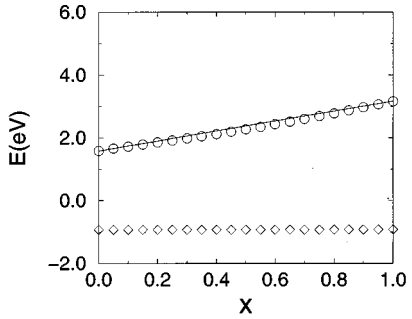

FIG. 1. Calculated valence-band splitting (open diamonds) and fundamental gap (open circles), together with band gap of Twadoski and co-workers (Ref. 18) solid line, as a function of the manganese concentration x in $\mathrm{Cd}_{1-x}\mathrm{Mn}_x\mathrm{Te}$.

$$E_{\mathrm{gap}}^{\mathrm{Cd}_{1-x}\mathrm{Mn}_x\mathrm{Te}}=E_{\mathrm{gap}}^{\mathrm{CdTe}}+x1587\ \ \mathrm{meV}, \tag{7}$$

where $E_{\mathrm{gap}}^{\mathrm{CdTe}}=1606$ meV. The second change relates to the splitting Δ of the valence band due to the spin-orbit interaction. Although the valence-band splitting of cubic MnTe has not yet been determined, the work of Nag[24] suggests that compounds with common anions have nearly equal values of Δ. Consequently, we assumed originally that $\Delta_{\mathrm{MnTe}}=\Delta_{\mathrm{CdTe}}$. This gave values of 0.016 and −0.0016 for λ^S and λ^A, respectively, in MnTe. The consequences of choosing different values of Δ_{MnTe} are discussed later in this section. The form factors for cubic MnTe are shown in Table I. It is worth noting that the effects of the $3d$ electrons in MnTe on the band structure do not appear explicitly in the present calculations; however, since the parameters we employ are deduced by fitting the resulting band structure to either *ab initio* calculations or spectroscopic data, which do include the effects of these $3d$ electrons, we have implicitly included the effects of these $3d$ electrons and hence the magnetic exchange coupling between the $3d$ electrons and the electrons in the the conduction and valence bands. It is the latter which determine the band gaps, bow factor, and effective masses of the electron and holes investigated in the present work.

Given the factors of the zinc-blende structure associated with CdTe and MnTe, the band structure of the range of alloys of $\mathrm{Cd}_{1-x}\mathrm{Mn}_x\mathrm{Te}$ was calculated using the virtual crystal approximation described in the previous section. In spite of its known limitations, the validity of the virtual crystal approximation for the $\mathrm{Cd}_{1-x}\mathrm{Mn}_x\mathrm{Te}$ structure in the energy range relevant to the present work has been established by other authors; see, e.g., Ref. 25.

Figure 1 gives the calculated fundamental gaps E_{gap} and Δ as a function of the manganese concentration. It can be

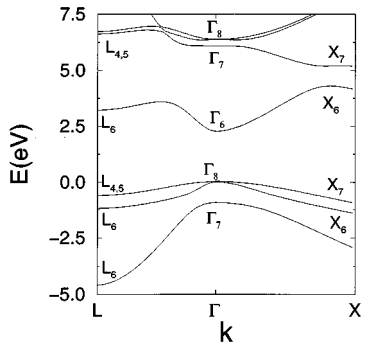

FIG. 2. Band structure of the DMS alloy $Cd_{0.5}Mn_{0.5}Te$.

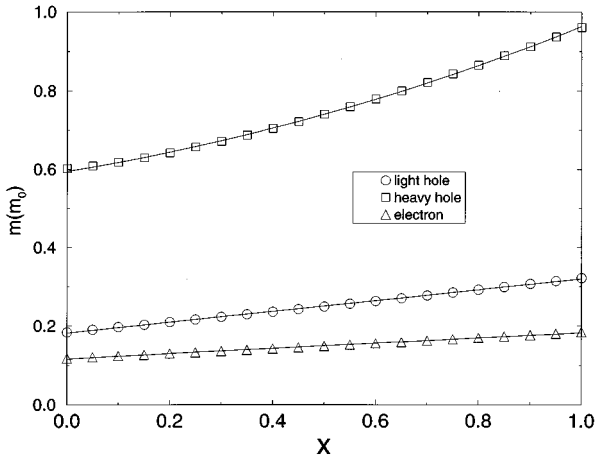

FIG. 3. Effective masses of the electron and light and heavy holes in $Cd_{1-x}Mn_xTe$ as a function of the manganese concentration x.

seen that the virtual crystal approximation suggests an optical bowing which, assuming the band gap $E_{\text{gap}}^{Cd_{1-x}Mn_xTe}$ can be expressed as a quadratic in x, i.e.,

$$E_{\text{gap}}^{Cd_{1-x}Mn_xTe}=(1-x)E_{\text{gap}}^{CdTe}+xE_{\text{gap}}^{MnTe}-bx(1-x), \tag{8}$$

gives a value for the bowing factor b of 0.45 eV. The linear expression of Twadoski and co-workers[18] in Eq. (7) and expressed as the solid line in Fig. 1 clearly gives no indication of optical bowing. This could be due to the difficulty in determining the manganese concentration accurately, with secondary-ion-mass spectroscopy, energy dispersive x-ray, etc., hence, the possibility of bowing in the alloy $Cd_{1-x}Mn_xTe$ must await experimental confirmation.

Figure 2 is a typical band structure for $Cd_{1-x}Mn_xTe$. In this example the manganese concentration $x=0.5$. The main difference with the band structure of CdTe is, of course, the increased fundamental gap; generally, however, the band structure remains topologically similar. The $3d$ electron bands are not given for the reasons described earlier in this section.

The effective masses of the electron, light, and heavy hole at a particular wave vector $\mathbf{k}$ are given by

$$m^*(\mathbf{k})=\left.\frac{\partial^2 E}{\partial k^2}\right|_{\mathbf{k}}, \tag{9}$$

and were calculated using a finite difference approximation. The effective masses along the [001] direction for CdTe were determined as $m_e^*=0.11$, $m_{\text{lh}}^*=0.18$, and $m_{\text{hh}}^*=0.60m_0$ and agree favorably with those commonly found in the literature.[26]

Figure 3 displays the effective masses as a function of the manganese concentration x. It is clear that the effective masses of all the carriers increase with x. Analysis has shown that the electron and light hole can be expressed as a linear function of x while the relationship with the heavy hole is quadratic. In particular, in units of the free electron mass m_0,

$$m_e^*=0.11+0.067x, \tag{10}$$

$$m_{\text{lh}}^*=0.18+0.14x, \tag{11}$$

$$m_{\text{hh}}^*=0.60+0.21x+0.15x^2. \tag{12}$$

We now consider the effects on the band gap, bow factor, and effective masses of a different choice for the spin-orbit parameter Δ_{MnTe}. Introduction of the spin-orbit interaction alters the band structure mainly through the removal of the six-fold degeneracy of the valence bands at the Γ point. In pseudopotential calculations, we can increase or decrease Δ_{MnTe} by changing the values of the parameters of λ^S and λ^A which in turn requires us to adjust the atomic form factors in order that the lowest conduction band and top valence bands maintain their good agreement with the experimental data and the results of *ab initio* calculations. Consequently there is no change in band gap of MnTe while the bow factor and the effective masses change very little. For example, if we choose $\Delta_{\text{MnTe}}=0.65$ eV, the changes of the bow factor and the effective masses (electron and holes) of MnTe are less than 0.02 eV and $0.01m_0$ respectively. Such changes, although small compared with our original values, indicate the level of uncertainty in these parameter values arising from the uncertainty in the value of Δ_{MnTe}.

IV. DISCUSSION

The consequences of increasing the electron and hole masses are wide ranging, particularly in the interpretation of optical spectroscopy experiments. Quantum-well structures formed from alternating layers of CdTe and the alloy $Cd_{1-x}Mn_xTe$ form type-I structures (at zero external magnetic field) with the electrons and holes both localized within the CdTe wells. Given that the electron and light- and heavy-hole masses are larger in the $Cd_{1-x}Mn_xTe$ barriers than the CdTe wells, this would mean that, for a fixed set of material parameters, higher one-particle energies will be deduced from envelope function calculations[27] compared with that assuming equal masses in the well and barrier. Consequently calculations based on the latter would need, in order to give agreement with experiment, to change one of the structural parameters, e.g., the well would have to be narrowed and/or the barrier height increased. This implies that hitherto, with

the effective masses being taken as the constant CdTe value, the well width may have been underestimated and/or the barrier height overestimated.

Furthermore, increasing effective masses leads to higher exciton binding energies and increased exciton localization,[28] which in turn will lead to higher magnetic polaron energies. Hence, theoretical models which assume that the effective masses take on the (lower) CdTe value will tend to underestimate the magnetic polaron energy.[29] The same is also true of the simpler one-particle neutral donor problem[30] in which the lower electron effective mass will lead to underestimations of the neutral donor binding energy.

V. CONCLUSION

The parameters characterizing the diluted magnetic semiconductor alloy $Cd_{1-x}Mn_xTe$ within the empirical pseudopotential scheme have been determined. The resulting band structures suggest optical bowing and have been used to calculate the effective masses of the electron and light and heavy holes along the [001] direction. The implications for spectroscopic experiments, of the increasing effective masses with alloy concentration, have been discussed.

ACKNOWLEDGMENTS

The authors would like to thank the University of Hull and the University of Leeds for financial support.

[1] J. M. Fatah, T. Piorek, P. Harrison, T. Stirner, and W. E. Hagston, Phys. Rev. B **49**, 10 341 (1994).
[2] W. E. Hagston, T. Stirner, J. P. Goodwin, and P. Harrison, Phys. Rev. B **50**, 5255 (1994).
[3] D. R. Yakovlev, *Festkörperprobleme*, Advances in Solid State Physics, Vol. 32, edited by U. Rössler (Vieweg, Braunschweig, 1992).
[4] T. Piorek, P. Harrison, and W. E. Hagston, Phys. Rev. B **52**, 14 111 (1995).
[5] S. Jackson, W. E. Hagston, P. Harrison, J. H. C. Hogg, J. E. Nicholls, B. Lunn, P. Devine, and S. Ali, Phys. Rev. B **49**, 13 512 (1994).
[6] T. Stirner, J. M. Fatah, R. G. Roberts, T. Piorek, W. E. Hagston, and P. Harrison, Superlattices and Microstructures **16**, 11 (1994).
[7] S. R. Jackson, J. E. Nicholls, W. E. Hagston, P. Harrison, T. Stirner, J. H. C. Hogg, B. Lunn, and D. E. Ashenford, Phys. Rev. B **50**, 5392 (1994).
[8] B. Kuhn-Heinrich, W. Ossau, T. Litz, A. Waag, and G. Landwehr, J. Appl. Phys. **75**, 8046 (1994).
[9] S.-K. Chang, A. V. Nurmikko, J.-W. Wu, L. A. Kolodziejski, and R. L. Gunshor, Phys. Rev. B **37**, 1191 (1988).
[10] G. Peter, E. Deleporte, J. M. Berroir, C. Delalande, J. M. Hong, and L. L. Chang, Phys. Rev. B **44**, 11 302 (1991).
[11] E. L. Ivchenko, A. V. Kavokin, V. P. Kochereshko, G. R. Posina, I. N. Uraltsev, D. R. Yakovlev, R. N. Bicknell-Tassius, A. Waag, and G. Landwehr, Phys. Rev. B **46**, 7713 (1992).
[12] M. L. Cohen and T. K. Bergstresser, Phys. Rev. **141**, 789 (1966).
[13] S.-H. Wei and A. Zunger, Phys. Rev. B **35**, 2340 (1987).
[14] S. Bloom and T. K. Bergstresser, Solid State Commun. **6**, 465 (1968).
[15] J. P. Walter, M. L. Cohen, Y. Petroff, and M. Balkanski, Phys. Rev. B **1**, 2661 (1970).
[16] D. J. Chadi, J. P. Walter, M. L. Cohen, Y. Petroff, and M. Balkanski, Phys. Rev. B **5**, 3058 (1972).
[17] D. E. Eastman, W. D. Grobman, J. L. Freeouf, and M. Erbudak, Phys. Rev. B **9**, 3473 (1974).
[18] A. Twadoski, M. Nawrochi, and J. Ginter, Phys. Status Solidi B **96**, 497 (1979).
[19] J. R. Chelikowsky and M. L. Cohen, Phys. Rev. B **14**, 556 (1976).
[20] J. W. Allen, G. Lucovsky, and J. C. Mikkelsen, Jr., Solid State Commun. **24**, 367 (1977).
[21] A. Pajaczkowska, Prog. Cryst. Growth Charact. **1**, 289 (1978).
[22] B. E. Larson, K. C. Hass, M. Ehrenreich, and A. E. Carlsson, Solid State Commun. **56**, 347 (1985).
[23] M. T. Czyzyk and M. Podgorny, Proc. Conf. Phys. **6**, 448 (1983).
[24] B. R. Nag, J. Appl. Phys. **77**, 4148 (1995).
[25] A. Kisiel, A.-I. Ali Dahr, P. M. Lee, G. Dalba, P. Fornasini, and E. Burattini, Phys. Rev. B **44**, 11 075 (1991).
[26] L. S. Dang, G. Neu, and R. Romestain, Solid State Commun. **44**, 1187 (1982).
[27] W. E. Hagston, P. Harrison, T. Piorek, and T. Stirner, Superlattices and Microstructures **15**, 199 (1994).
[28] P. Harrison, F. Long, and W. E. Hagston, Superlattices and Microstructures (to be published).
[29] T. Stirner, P. Harrison, W. E. Hagston, and J. P. Goodwin, Phys. Rev. B **50**, 5713 (1994).
[30] W. E. Hagston, P. Harrison, and T. Stirner, Phys. Rev. B **49**, 8242 (1994).